Nonequilibrium Thermodynamics and the Optimal Path to Turbulence in Shear Flows

Antonios Monokrousos,[1,*] Alessandro Bottaro,[2] Luca Brandt,[1] Andrea Di Vita,[2] and Dan S. Henningson[1]

[1]*Linné Flow Centre, SeRC, KTH Mechanics, SE-100 44 Stockholm, Sweden*

[2]*DICAT, Università di Genova, Via Montallegro 1, 16145 Genova, Italy*

(Received 5 December 2010; published 29 March 2011)

We determine the initial condition on the laminar-turbulent boundary closest to the laminar state using nonlinear optimization for plane Couette flow. Resorting to the general evolution criterion of nonequilibrium systems we optimize the route to the statistically steady turbulent state, i.e., the state characterized by the largest entropy production. This is the first time information from the fully turbulent state is included in the optimization procedure. We demonstrate that the optimal initial condition is localized in space for realistic flow domains.

DOI: 10.1103/PhysRevLett.106.134502 PACS numbers: 47.27.Cn, 05.70.Ln, 47.20.Ky, 47.27.nb

The transition from laminar to turbulent flow is still a challenging problem despite the fact that our understanding has increased significantly in recent years [1–3]. In canonical shear flows (pipe, channel, and Couette flows) transition is typically subcritical and initial perturbations of finite amplitudes are necessary.

This Letter is about the computation and nature of the smallest disturbances that most quickly trigger turbulence in linearly stable shear flows. This is relevant both for our understanding of the flow physics as well as designing effective control strategies [4]. To do this, we optimize the trajectory of the system with respect to the general evolution criterion [5] of nonequilibrium thermodynamics. The criterion has been used successfully in a wide range of applications, shock waves [6], biology [7], climate research [8,9], and nuclear fusion [10], although never, thus far, in the search for optimal turbulence-triggering disturbances.

Recent progress in the understanding of subcritical transition to turbulence in shear flows was made using the nonlinear concept of edge state, originating from dynamical systems' theory. Edge state refers to the flow regime reached asymptotically by phase-space trajectories visiting neither the turbulent nor the laminar state. It is an unstable flow state, yet embedded exact coherent states have been identified numerically: steady states, traveling waves, and periodic orbits (see [1–3] and references therein).

Here, we wish to determine the most dangerous perturbation leading to the turbulent state. Two concepts are key to our analysis: (i) optimal initial condition and (ii) the target final state of the flow. Optimally growing perturbations (in energy norm) have been considered extensively within the linear framework [11]. This nonmodal approach has been able to explain the physical mechanisms responsible for energy growth in shear flows and, together with weakly nonlinear models such as secondary instability analysis, contributed to drawing a plausible picture of the early stages of the transition process. However, the later stages are inherently nonlinear and linear theory fails. Nonlinear optimization in reduced-order subspaces has been presented before [12–14], while only very recently researchers considered fully nonlinear optimization, without targeting the turbulent state [15,16]. In the former study [15], the authors use the full Navier-Stokes equations to show how nonlinearity can change the optimal which emerges from a linear transient growth analysis in pipe flow at subcritical condition. The optimal initial condition obtained is three dimensional and shows signs of localization. As reported in [15], a more extensive optimization adopting larger flow domains would provide confirmation and formidable extension of the results in that work. Here, we take this step further and confirm the prediction that the optimal is fully localized in extended flow domains. Furthermore, we include the fully turbulent state into the optimization procedure and manage to bridge the gap between the optimization initial amplitude and the actual transition threshold [15].

To take this step, it is crucial to select a metric for the definition of the final flow state. Here we resort to thermodynamics considerations to select the objective of our optimization, unlike previous studies where the disturbance kinetic energy has been used. The theory is tested on the simple case of plane Couette flow, a flow stable for all values of the Reynolds $\mathrm{Re} = \frac{Uh}{\nu}$, where $\pm U$ and h are the velocity at each wall and the channel half-width, with ν the kinematic viscosity. Time is therefore reported in units of h/U.

All shear flows by definition are not in equilibrium with their environment since there is continuous energy exchange through the walls. However, the Navier-Stokes equations can be viewed as a special case of the Boltzmann equation for systems for which the local thermodynamic equilibrium assumption is valid [17]. Glansdorff and Prigogine [5] demonstrated that for time invariant boundary conditions the system eventually reaches a statistically steady state. When dissipation is dominant (low Reynolds number) the system goes back to the laminar state, while when inertia dominates

(high values of Re) the turbulent state ensues. A fully developed flow, from the standpoint of thermodynamics, is a statistically steady state. A chaotic turbulent flow is indeed characterized by steady values of time-averaged quantities, such as fluctuations and dissipation. The approach of the fluid system to a statistically steady state is central to the theory presented here [18].

The general evolution criterion implies that certain quantities obtain extreme values once the statistically steady state is reached. It has been recently demonstrated [17] that this leads to Malkus heuristic principle [18]: a viscous, turbulent, incompressible Couette flow in statistically steady state with assigned mean velocity maximizes the total rate of viscous dissipation. To determine the optimal initial condition leading to turbulent flow, we employ Lagrangian optimization where the functional $\mathcal{L}$ to maximize consist of an objective function and two constraints (the Navier-Stokes equations and the energy level of the initial disturbance), i.e.,

$$\mathcal{L} = \mathcal{J} - \int_0^T [(\mathbf{u}^*, \mathrm{NS}(\mathbf{u})) + (p^*, \nabla \cdot \mathbf{u})_E] dt - \lambda(\|\mathbf{u}(0) - \mathbf{U}\|_E^2 - \epsilon_0), E \quad (1)$$

with the subscript E denoting the energy inner product, i.e., the integral over the whole domain. In the above, $\mathbf{u}^*$, p^*, and λ are the Lagrange multipliers, i.e., the adjoint variables, NS the nonlinear Navier-Stokes equations, and ϵ_0 the kinetic energy of the perturbation at $t = 0$; $\mathbf{u}$ is the velocity vector and $\mathbf{U}$ the Couette base flow. Since the system under consideration is chaotic we will maximize the average value of the functional, integrating over a sufficiently long time interval. As introduced above, the objective function is the time-averaged dissipation

$$\mathcal{J} = \frac{1}{T} \int_0^T \frac{1}{\mathrm{Re}} (\nabla \mathbf{u} : \nabla \mathbf{u}) dt, \quad (2)$$

with T the final observation time. Maximizing the time integral of the entropy production implies that we also obtain the fastest route to turbulence for any given value of the initial energy ϵ_0. Variations of the Lagrangian provide the gradient of the objective function with respect to variation of the initial condition $\mathbf{u}_0$. The gradient $\nabla_{\mathbf{u}(0)} \mathcal{L} = \mathbf{u}^*(0)$ is obtained by forward time integration of the Navier-Stokes equations and backward integration of the adjoint system, the latter containing $-1/(T\mathrm{Re})\nabla^2 \mathbf{u}$ a source term stemming from the definition of $\mathcal{J}$.

This forcing term is stochastic when the flow has become turbulent. It can change significantly for very small variations of the initial conditions, as it occurs typically in chaotic flows. As a consequence, the update of the initial condition can be significant even in the proximity of an optimal. Therefore to improve convergence we include a relaxation term for each update of the initial guess

$$\mathbf{u}(0)^{n+1} = (1 - \sigma)\mathbf{u}^*(0)^n + \sigma \mathbf{u}(0)^n. \quad (3)$$

Close to convergence, the relaxation term gives an ensemble average of the different initial conditions, since the values of the objective function (i.e., the statistics of the turbulent state) are basically constant. A fully converged initial condition can be obtained more easily for the smaller values of ϵ_0 considered, when the flow never becomes turbulent and just above the minimum value ϵ_{0T} of the initial energy for which a turbulence state can be established. Larger initial amplitudes yield a very noisy optimization. Indeed, we first optimize for large values of the initial energy and gradually reduce the value of ϵ_0 to be sure to target the final turbulent state. Typically we perform between 50 and 100 iterations for each level of initial energy.

In Fig. 1 the energy threshold necessary to reach a turbulent state is displayed for each initial condition found by the optimization procedure in the largest domain considered. Each of these initial conditions is defined by the energy level ϵ_0 used in the Lagrangian $\mathcal{L}$ [see Eq. (1)]. The threshold level is determined by a classic bisection procedure with an accuracy of five digits. The straight line is a guide to the eye and indicates equal values of the energy on the axis. For the largest ϵ_0 considered, one can reduce the amplitude of the initial condition and still reach the turbulent state. When decreasing the constraint on the initial energy, we reach a value ϵ_{0T} below which the flow

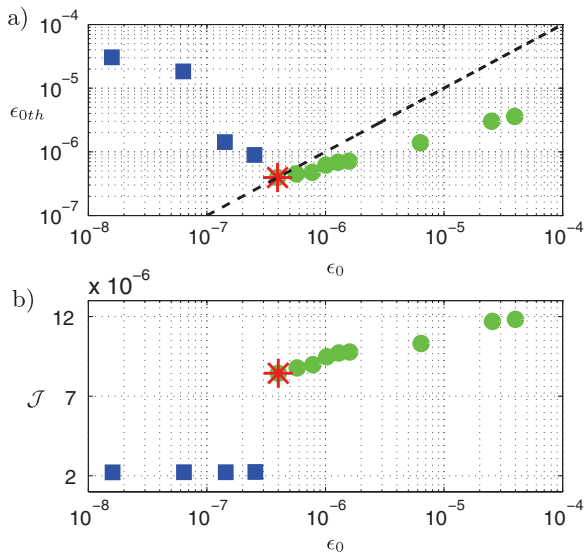

FIG. 1 (color online). (a) Energy threshold ($\epsilon_{0\mathrm{th}}$) to reach a turbulent state and (b) viscous dissipation rate (objective function $\mathcal{J}$) versus the energy amplitude ϵ_0 used to determine the shape of the optimal initial condition. The energy for transition is computed by applying bisection to each optimal initial condition to scale its amplitude. The square blue symbols pertain to initial conditions determined with laminar flow at final time $T = 300$. Data for Couette flow at $\mathrm{Re} = 1500$, domain size $4\pi \times 2 \times 2\pi$ with resolution $128 \times 73 \times 64$ grid points in the streamwise, wall-normal, and spanwise direction, respectively.

remains laminar for any $t < T$. This is indeed the nonlinear optimal initial condition of smallest amplitude leading to a statistically steady turbulent flow.

For values of the initial energy lower than ϵ_{0T}, where turbulent flow is not reached during the optimization procedure, the initial condition must be scaled up by a factor of about 4 or 5 to trigger transition, similarly to what was obtained in [15]. Previous optimizations [15,16] in fact considered highly distorted yet laminar flows (in the latter work owing to the relatively short optimization interval). The threshold for transition is then computed with a bisection procedure to find the laminar-turbulent boundary. The initial condition of critical energy ϵ_{0T} obtained with the present procedure is just above the boundary and its energy is lower than that obtained from nonlinear optimization of a laminar flow. In addition, having a turbulent state as final target gives a lower threshold for transition with optimals computed above ϵ_{0T} than below ϵ_{0T}. For $\epsilon_0 \to 0$ we would retrieve the linear optimals which cannot induce turbulence alone. Therefore a fully nonlinear optimization, including information from the fully turbulent state, is indeed indispensable if the target is the complete transition process. Note that we have also performed a series of simulations using the time integral of the disturbance kinetic energy as objective function. Although the results are qualitatively the same, dissipation provides a lower threshold amplitude for transition, about 5% smaller. More importantly, we obtain better convergence with dissipation as objective function; for the lowest Reynolds numbers considered we could not obtain converged results when using the disturbance kinetic energy. Note also that previous studies used the kinetic energy at final time rather then the time integral: this can explain improved convergence with our approach.

We performed optimization for a combination of 4 different values of the Reynolds numbers, $\mathrm{Re} = [500, 750, 1000, 1500]$, three difference box sizes, $[2\pi \times 2 \times \pi]$, $[4\pi \times 2 \times \pi]$, $[4\pi \times 2 \times 2\pi]$, and final optimization time $T \in [200, 400]$. It turned out to be more difficult to obtain converged solutions for the lowest Reynolds number considered. This is because the method relies on the concept of statistically steady state which implies a well-developed turbulent field. This is not the case at lower values of the Reynolds number where turbulence has a transient nature. Furthermore, sufficient time is needed to reach a final turbulent flow. The optimal initial condition obtained with different optimization times T is displayed in Fig. 2. The variations are marginal for the cases considered here for final times beyond $T = 300$, as quantified by the maximum of the velocity amplitude in the whole domain in Fig. 2(e). The results are therefore independent of T, the objective function has reached an asymptotic value, and we have indeed optimized the route to the turbulent state.

For smaller domains and lower Reynolds number the edge trajectories visit some steady solution before the final breakdown to turbulence. This is not the case for the largest

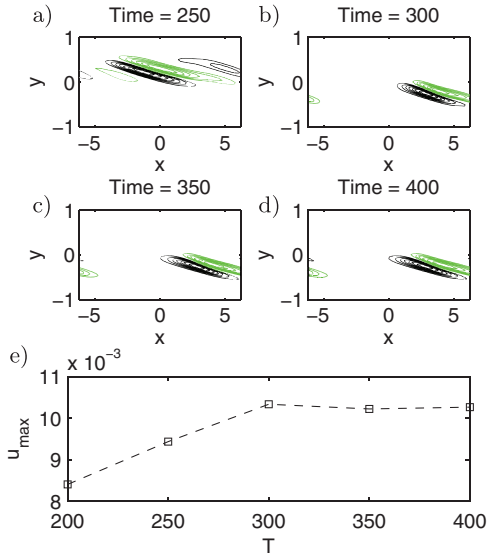

FIG. 2 (color online). Optimal initial condition at the minimum threshold level ϵ_{0T} for different values of the final optimization time: (a) $T = 250$, (b) $T = 300$, (c) $T = 350$, (d) $T = 400$. The plot displays the streamwise velocity component in the wall-normal (x, y) plane at $z = \pi/2$. The subplot (e) shows the maximum of the velocity amplitude in the whole domain versus the final optimization time T. The data pertain to the largest box size considered, $\mathrm{Re} = 1500$.

domain and higher Re considered, where a chaotic behavior is observed near the edge trajectory. Evidence for this is provided in Fig. 3(a) where the evolution of the rms values of the wall-normal velocity perturbation is displayed for two cases.

The optimal trajectory to the turbulent state is visualized in physical space in Fig. 4. The perturbation at $t = 0$ is strongest in the cross-stream velocity components and,

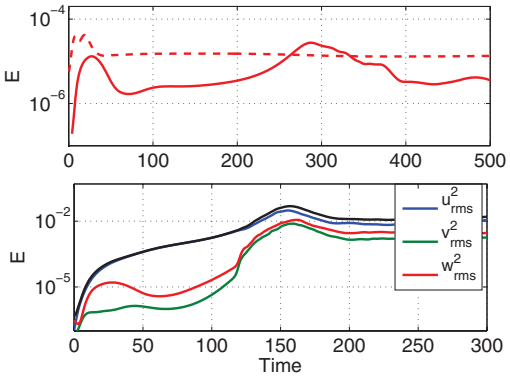

FIG. 3 (color online). (a) The red solid line shows the edge trajectory for minimum energy threshold ϵ_{0T} at $\mathrm{Re} = 1500$ and domain size $4\pi \times 2 \times 2\pi$. The red dashed line indicates the edge trajectory at $\mathrm{Re} = 500$ with domain size $2\pi \times 2 \times \pi$. The energy of the wall-normal velocity perturbation is displayed. (b) Evolution of the energy in time for the nonlinear optimal discussed in Fig. 1 for $\epsilon_0 = \epsilon_{0T}$.

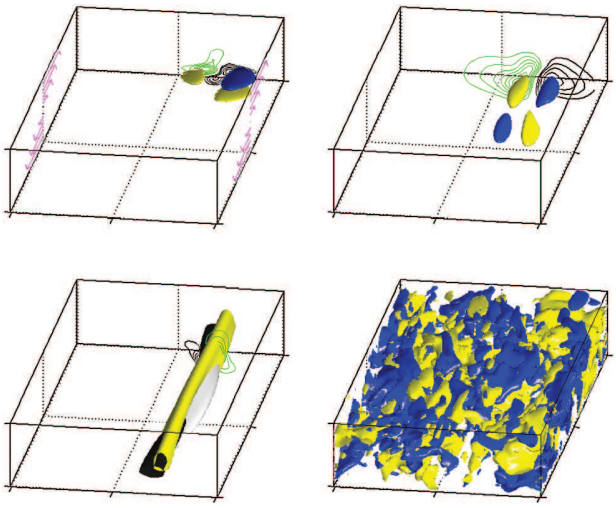

FIG. 4 (color online). Optimal initial condition at the threshold level ϵ_{0T}, visualized through isosurfaces of positive and negative streamwise velocity perturbation, shown with light (yellow) and dark (blue) color. Contour lines show positive and negative spanwise velocity at $x = 1.5\pi$. The base flow is indicated by the arrows along the sides in (a). Re $= 1500$, domain size $4\pi \times 2 \times 2\pi$. The isosurface level is 65% of the maximum value of each component: (a) $u^2_{\max} = 2.89 \times 10^{-5}$, (b) $u^2_{\max} = 2.89 \times 10^{-5}$, (c) $u^2_{\max} = 2.09 \times 10^{-3}$, (d) $u^2_{\max} = 2.07 \times 10^{-1}$.

most interestingly, it appears localized in all three spatial directions. Nonlinearity is active where the amplitude is locally large and this is not always reflected by the total energy, which is a global measure. The initial evolution of the disturbance is reported in Figs. 4(b) and 4(c) while the behavior of the integral energy is shown in Fig. 3(b). The initial disturbance is inclined against the mean shear to extract more energy from the base flow via the Orr-mechanism At time $t = 10$ the disturbance is upright and still localized.

Transition is initiated by a pair of streamwise vortices that generate a single bent streak [19], see Fig. 4(c). The slow growth of the streak is associated to a decay of the cross-stream velocity components [see Fig. 3(b)]. However, once the streak reaches a sufficient amplitude at $t \approx 70$, secondary instability sets in as spanwise oscillations induced by a staggered pattern of vorticity. Rapid breakdown to turbulence is then observed to occur at $t \approx 130$.

To determine the initial condition of minimum energy leading to laminar-turbulent transition in plane Couette flow we have resorted to thermodynamics considerations. Using the general evolution criterion we have optimized the route to the statistically steady state the system wants to reach: this is the state of maximum entropy production and coincides with the turbulent state for large enough values of the Reynolds number and of the initial perturbation energy. Nonlinear optimization is needed to determine this optimal initial condition and the energy threshold below which turbulence cannot ensue. For realistic domain sizes the optimal initial condition is localized in the three spatial directions. The transition path is characterized by the occurrence of a single bent velocity streak whose oscillations increase rapidly at breakdown. Although computationally expensive, the approach proposed is not limited to simple flows, and the next step is to extend the present results to flows that are inhomogeneous in the streamwise direction.

The authors acknowledge Carlo Cossu for fruitful discussions. Computer time provided by SNIC (Swedish National Infrastructure Centre) is gratefully acknowledged.

*antonios@mech.kth.se

[1] B. Hof, C. W. H. van Doorne, J. Westerweel, F. T. M. Nieuwstadt, H. Faisst, B. Eckhardt, H. Wedin, R. R. Kerswell, and F. Waleffe, Science **305**, 1594 (2004).
[2] B. Eckhardt, Annu. Rev. Fluid Mech. **39**, 447 (2007).
[3] T. Mullin, Annu. Rev. Fluid Mech. **43**, 1 (2011).
[4] G. Kawahara, Phys. Fluids **17**, 041702 (2005).
[5] P. Glansdorff and I. Prigogine, Physica (Amsterdam) **30**, 351 (1964).
[6] E. Rebhan, Phys. Rev. A **42**, 781 (1990).
[7] D. Juretic and P. Zupanovic, Comp. Biol. Chem. **27**, 541 (2003).
[8] G. W. Paltridge, Nature (London) **279**, 630 (1979).
[9] H. Ozawa, A. Ohmura, R. D. Lorenz, and T. Pujol, Rev. Geophys. **41**, 1 (2003).
[10] A. DiVita and M. Brusati, Plasma Phys. Controlled Fusion **37**, 1075 (1995).
[11] P. J. Schmid and D. S. Henningson, *Stability and Transition in Shear Flows* (Springer, New York, 2001).
[12] S. C. Reddy and D. S. Henningson, J. Fluid Mech. **252**, 209 (1993).
[13] D. Viswanath and P. Cvitanovic, J. Fluid Mech. **627**, 215 (2009).
[14] Y. Duguet, L. Brandt, and B. R. J. Larsson, Phys. Rev. E **82**, 026316 (2010).
[15] C. C. T. Pringle and R. R. Kerswell, Phys. Rev. Lett. **105**, 154502 (2010).
[16] S. Cherubini, P. De Palma, J.-C. Robinet, and A. Bottaro, Phys. Rev. E **82**, 066302 (2010).
[17] A. Di Vita, Phys. Rev. E **81**, 041137 (2010).
[18] W. V. R. Malkus, J. Fluid Mech. **1**, 521 (1956).
[19] C. Cossu, M. Chevalier, and D. S. Henningson, in *Proceedings of the Seventh IUTAM Symposium on Laminar-Turbulent Transition* (Springer, Berlin, Germany, 2010), Vol. 18, pp. 129–134.